Journal of Mathematical Chemistry 21 (1997) 305–321

Travelling waves in an open quadratic autocatalytic chemical system

A.B. Finlayson and J.H. Merkin
Department of Applied Mathematical Studies, University of Leeds, Leeds LS2 9JT, UK

Received 19 November 1996; revised 5 May 1997

The travelling waves that are initiated in an autocatalytic reaction–diffusion system with quadratic rate law are considered. The system is modelled on the basis of a continuous-flow, unstirred reactor. The model is used to determine whether any of the complex structures reported for cubic autocatalytic reaction–diffusion systems can also be observed in the quadratic model. This is found not to be the case. The range of behaviour of the quadratic model is much less complex, with only front waves being initiated under the necessary conditions, which are established. There are, however, some unusual transient features to be found after the initial passage of the wave front.

1. Introduction

A way of studying the spatio-temporal behaviour of reaction–diffusion systems is through the continuous-flow, unstirred reactor (CFUR). In this reactor a continuous supply of fresh reactants is achieved in a way that does not interfere with the transport processes by molecular diffusion. A reaction zone is created, usually involving a gelled medium, which is contained between impermeable walls at its ends. This reaction region is also in contact with a reservoir from which fresh reactants can be drawn, by diffusion through permeable membranes for example, and into which reaction products can be removed from the reaction zone. The chemical composition of the reservoir is kept constant by continuous flow, thus enabling steady states and other indefinitely sustainable structures to be observed.

Here we consider a simple model for the CFUR in which we assume that spatial variations occur only in a direction 'along' the reactor, i.e., can be represented by the single spatial variable x. We also assume that the exchange processes between the reaction zone and the reservoir can be modelled by linear diffusive interchange terms. We consider the case of a simple prototype reaction within the CFUR which is isothermal and given purely by the quadratic autocatalytic kinetics

$$A + B \to 2B, \quad \text{rate } kab \tag{1}$$

(where a and b are the concentrations of reactant A and autocatalyst B, respectively, and k is the rate constant).

Furthermore, we are concerned here with the possible reaction–diffusion travelling waves that can be initiated in the reactor and to this end we assume that reactant A has an initially uniform concentration a_0, the same concentration of A within the reservoir. We also assume that autocatalyst B is introduced into the reaction zone locally at the end $x = 0$ and, for simplicity, we assume that there is no autocatalyst supplied to the reaction zone from the reservoir.

Finally, we take the reaction zone to be sufficiently long for any travelling waves to be fully formed well before the influence of the end at $x = l$ is felt, i.e., in effect assuming the reaction zone to be 'semi-infinite' in extent. A schematic representation of our CFUR model is shown in figure 1.

These considerations lead to the equations and initial and boundary conditions

$$\frac{\partial a}{\partial t} = D_A \frac{\partial^2 a}{\partial x^2} + M_A(a_0 - a) - kab, \tag{2}$$

$$\frac{\partial b}{\partial t} = D_B \frac{\partial^2 b}{\partial x^2} - M_B b + kab, \tag{3}$$

where D_A, D_B and M_A, M_B are the diffusion coefficients and mass transfer coefficients of reactant A and autocatalyst B respectively. Initially we have

$$\begin{aligned} a(x, 0) &= a_0, \\ b(x, 0) &= b_0 g(x), \end{aligned} \tag{4}$$

where $g(x)$ represents some local input of B, i.e., $g(x)$ is zero outside some finite subinterval $[0, \sigma]$ of $[0, +\infty]$ and b_0 is a positive constant. The boundary conditions are

$$a \to a_0, \quad b \to 0, \quad \text{as } x \to \infty, \ t > 0, \tag{5}$$

and zero flux on $x = 0$.

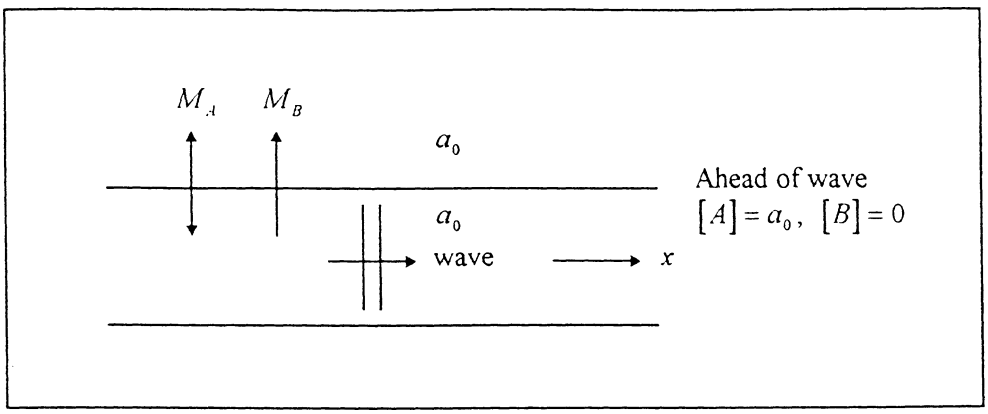

Figure 1. Schematic representation of the CFUR modelled by equations (2) and (3).

A model very similar to that given by equations (2)–(5), with the only difference being that the prototype kinetics are given by cubic autocatalysis, has already received considerable attention. Pearson and co-workers [4,11,14] have shown that complex spatio-temporal structures can arise in their model, with the formation, extinction and self-replication of spots (or patterns) being observed. Their work is concerned primarily with finite domains (in both one and two dimensions) and required unequal diffusivities for the two chemical species. Petrov et al. [12] have also considered the cubic autocatalysis case, again on a finite (one-dimensional) domain and with unequal diffusion coefficients for species A and B. They showed that the model could exhibit wave reflection from (zero flux) boundaries as well as wave splitting for suitable choices of the parameters. The cubic autocatalysis model has also been treated by Merkin et al. [8,9] and Merkin and Sadiq [10]. This work was concerned essentially with a semi-infinite domain (as is the case in the present model) and with equal diffusion coefficients. They considered the possible travelling waves that could be initiated and showed that both front waves and pulse waves could form. However, the most unusual feature of their study was in showing that, for suitable parameter values, the initial passage of a front wave could leave behind a region where there was spatio-temporal chaos, with this then being sustained indefinitely. The appearance of these complex spatio-temporal structures have also been confirmed in a recent paper by Rasmussen et al. [13]. More recently, Jones and O'Brien [3] have investigated this model numerically in two dimensions, paying particular attention to the development of the instabilities that can occur in both plane and axisymmetric waves.

Here we are concerned with the case of quadratic autocatalysis to see if any of the complex structures reported for cubic autocatalysis can also be observed in our model. We find that this is not the case. The range of behaviour in our model is much less complex, with only front waves being initiated, though these can generate some, perhaps unexpected, transient features after their initial passage, with pulse-like behaviour in B and ramp-like behaviour in A being seen.

We simplify equations (2) and (3) by making them dimensionless through the introduction of the substitutions below, following [8–10]:

$$a = a_0\overline{a}, \quad b = a_0\overline{b}, \quad \overline{t} = M_A t, \quad \overline{x} = \sqrt{\frac{M_A}{D_A}}x,$$

to give (on dropping the bars for convenience)

$$\frac{\partial a}{\partial t} = \frac{\partial^2 a}{\partial x^2} + 1 - a - \mu ab, \tag{6}$$

$$\frac{\partial b}{\partial t} = \delta\frac{\partial^2 b}{\partial x^2} - \phi b + \mu ab \tag{7}$$

on $0 < x < \infty$, $t > 0$, where $\mu = ka_0/M_A$, $\delta = D_B/D_A$, $\phi = M_B/M_A$. Note also that μ is the only parameter that depends on the reservoir concentration, a_0, of reactant A and hence changes in μ can be directly related to changes in this concentration.

The initial and boundary conditions become

$$a = 1, \quad 0 < x < \infty, \ t = 0, \tag{8}$$

and

$$b = \begin{cases} \beta_0 g(x), & 0 \leqslant x < \sigma, \\ 0, & \text{otherwise}, \end{cases} \quad t = 0, \tag{9}$$

where σ defines the local input region and $\max_{0 \leqslant x < \sigma} \{g(x)\} = 1$ with $g(x)$ being smooth and non-negative and $\beta_0 = b_0/a_0$.

We are considering waves propagating only in the positive x-direction and apply no-flux boundary conditions at $x = 0$, namely,

$$\frac{\partial a}{\partial x} = 0, \quad \frac{\partial b}{\partial x} = 0 \quad \text{at } x = 0. \tag{10}$$

with

$$a \to 1, \quad b \to 0 \quad \text{as } x \to \infty, \ t > 0. \tag{11}$$

The above model assumes different mean transfer coefficients for the chemical species A and B. This assumption can be removed and equal mass transfer coefficients allowed for if we also introduce the linear termination step

$$B \to \text{inert}, \quad \text{rate } k_t b,$$

into our kinetic mechanism. With this extra step (and $M_A = M_B$) we now have that

$$\phi = \frac{M_A + k_t}{M_A}.$$

The type of chemical reactions which are modelled by the reaction scheme (1) generally involve species A and B which have a similar molecular size. In such cases little variation in their diffusion rates is found and it is reasonable to consider the species A and B as having equal diffusion coefficients; thus we can assume $D_A = D_B$, i.e., $\delta = 1$. This is the case we shall concentrate on in the following discussion. We start by giving a brief summary of the kinetics of equations (6) and (7).

2. Kinetics

The dynamical behaviour of the kinetics of equations (6) and (7) is described by the ordinary differential equations

$$\frac{\mathrm{d}a}{\mathrm{d}t} = 1 - a - \mu ab, \tag{12}$$

$$\frac{\mathrm{d}b}{\mathrm{d}t} = \mu ab - \phi b. \tag{13}$$

The stationary states of the kinetic equations (12) and (13) are easily shown to be

$$a_s = 1, \quad b_s = 0 \tag{14}$$

and

$$a_s = \frac{\phi}{\mu}, \quad b_s = \frac{\mu - \phi}{\mu\phi}. \tag{15}$$

We note that stationary state (15) requires $\mu \geqslant \phi$ for a physically acceptable solution ($b_s \geqslant 0$).

The linear stability of these stationary states is readily determined. We find that (14) is stable (node) for $\mu < \phi$ and unstable (saddle point) for $\mu > \phi$. Stationary state (15) is unstable (saddle point) for $\mu < \phi$ and stable for $\mu > \phi$, being a node for all μ if $\phi \leqslant 1$ and, for $\phi > 1$, a node for $\phi < \mu < \mu_-$, a focus for $\mu_- < \mu < \mu_+$ and a node for $\mu > \mu_+$, where

$$\mu_\pm = 2\left(\phi^2 \pm \phi^{3/2}\sqrt{\phi - 1}\right).$$

The bifurcation diagram in figure 2 illustrates the ranges of stability and instability.

3. A priori bounds

Before considering the possible permanent form travelling waves that can be initiated in the open quadratic autocatalytic system, we establish a priori bounds for the solutions of the initial-value problem (6)–(11).

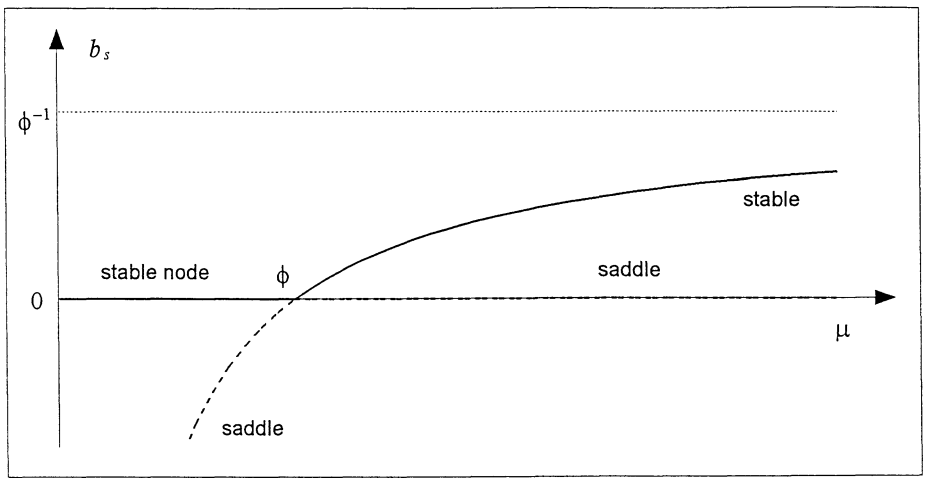

Figure 2. Bifurcation diagram (a plot of b_s against μ) to show the regions of stability and instability of the stationary states (a_s, b_s), where —— represents a stable and - - - - represents an unstable stationary state.

3.1. A priori bounds for a

It is readily established, Smoller [16], Britton [2], and taking due regard of the behaviour as $x \to \infty$ along the lines described by Merkin et al. [7] that

$$a \geqslant 0, \quad b \geqslant 0 \quad \text{on } 0 \leqslant x < \infty,\ t > 0. \tag{16}$$

We next consider the linear operator

$$N[u] = u_t - u_{xx} - 1 + u \quad \text{on } 0 \leqslant x < \infty,\ t > 0, \tag{17}$$

with

$$u_x(0,t) = 0.$$

Then for $\overline{u} = 1,\ \underline{u} = a$

$$N[\overline{u}] = 0, \quad N[\underline{u}] = -\mu a b \leqslant 0 \quad \text{on } 0 \leqslant x < \infty,\ t > 0, \tag{18}$$

from (17). Also, $\underline{u}(x,0) \leqslant 1 \leqslant \overline{u}(x,0)$, $\underline{u}_x(0,t) \leqslant \overline{u}_x(0,t)$. Hence $\underline{u} = a,\ \overline{u} = 1$ are a regular subsolution and supersolution of operator (17) respectively, so that by the scalar comparison theorem for linear parabolic operators,

$$0 \leqslant a(x,t) \leqslant 1 \quad \text{on } 0 \leqslant x < \infty,\ t > 0. \tag{19}$$

3.2. A priori bounds for b

Next we consider the operator

$$N[u] = u_t - \delta u_{xx} - (\mu - \phi)u \quad \text{on } 0 \leqslant x < \infty,\ t > 0, \tag{20}$$

with

$$u_x(0,t) = 0.$$

For $\underline{u} = b$, $\overline{u} = b_0 \mathrm{e}^{(\mu-\phi)t}$

$$N[\underline{u}] = \mu b(a-1) \leqslant 0, \quad N[\overline{u}] = 0 \quad \text{on } 0 \leqslant x < \infty,\ t > 0,$$

from (19). Also, $\underline{u}(x,0) = b_0 g(x) \leqslant b_0 = \overline{u}(x,0)$ and $\underline{u}_x(0,t) \leqslant \overline{u}_x(0,t)$. Hence $\underline{u}$ and $\overline{u}$ are a regular subsolution and supersolution respectively of operator (20). Hence

$$0 \leqslant b(x,t) \leqslant b_0 \mathrm{e}^{(\mu-\phi)t} \quad \text{for } 0 \leqslant x < \infty,\ t \geqslant 0. \tag{21}$$

Hence the solution is bounded uniformly for all finite t, which, from Smoller [16] (theorem 14.4) guarantees uniqueness and global existance. Expression (21) also leads to the following.

3.3. *Necessary conditions for the existence of travelling waves*

For the case $\mu < \phi$, condition (21) shows that $b(x,t) \to 0$ as $t \to \infty$ uniformly in x. Also, with $b \equiv 0$, equation (6) gives that $a \to 1$ as $t \to \infty$. Also, with $\phi = \mu$, equation (7) gives

$$\frac{\partial b}{\partial t} - \delta \frac{\partial^2 b}{\partial x^2} = \mu(a-1)b \leqslant 0.$$

Then, using the maximum principle for the diffusion equation, it follows that travelling waves will not be initiated when $\mu = \phi$. Hence, we conclude that a necessary condition for travelling waves to exist is that

$$\mu > \phi. \tag{22}$$

Significant insights into the nature of the solution to the initial-value problem (6)–(11) can be gained from a consideration of the travelling waves of permanent form that are sustainable by these equations, as these can form the large time behaviour of the system. This is what we discuss next.

4. Permanent form travelling waves

We now establish properties of the permanent form travelling waves in the open quadratic autocatalytic system. We put $a = a(y)$, $b = b(y)$, where y is the travelling co-ordinate given by $y = x - \nu t$ with ν being the constant wave speed. For these travelling waves to emerge as the long time solutions to our initial-value problem we require $\nu > 0$. Equations (6) and (7) then give

$$\frac{\mathrm{d}^2 a}{\mathrm{d}y^2} + \nu \frac{\mathrm{d}a}{\mathrm{d}y} + 1 - a - \mu ab = 0, \tag{23}$$

$$\frac{\mathrm{d}^2 b}{\mathrm{d}y^2} + \nu \frac{\mathrm{d}b}{\mathrm{d}y} + \mu ab - \phi b = 0 \tag{24}$$

on $-\infty < y < \infty$, with boundary conditions

$$a \to 1, \quad b \to 0 \quad \text{as } y \to \infty. \tag{25}$$

We require a non-negative (from (19) and (21)), non-trivial solution to equations (23) and (24). In addition, we require conditions to be uniform at the rear of the wave. This leads to, from (14) and (15) that

$$a \to \frac{\phi}{\mu}, \quad b \to \frac{\mu - \phi}{\mu\phi} \quad \text{as } y \to -\infty, \tag{26}$$

which indicates that a front wave is generated, or that

$$a \to 1, \quad b \to 0 \quad \text{as } y \to -\infty, \tag{27}$$

which indicates a pulse wave.

From (22) we need only consider the case when $\mu \geqslant \phi$. We start by considering the special case when $\phi = 1$.

4.1. Solution for $\phi = 1$

With $\phi = 1$ (and $\mu \geqslant 1$) we can add equations (23) and (24) to get a linear equation for $a + b$. The only solution to this equation which remains bounded as $|y| \to \infty$ and satisfies boundary condition (25) is $a + b \equiv 1$. This leads to the single equation

$$\frac{\mathrm{d}^2 b}{\mathrm{d}y^2} + \nu \frac{\mathrm{d}b}{\mathrm{d}y} + \mu(1-b)b - b = 0. \tag{28}$$

Multiplying equation (28) by $\mathrm{d}b/\mathrm{d}y$ and applying $\int_{-\infty}^{\infty} \ldots \mathrm{d}y$ leads to

$$\nu \int_{-\infty}^{\infty} \left(\frac{\mathrm{d}b}{\mathrm{d}y}\right)^2 \mathrm{d}y = \int_{b_{-\infty}}^{b_\infty} \left(b - \mu b + \mu b^2\right) \mathrm{d}b. \tag{29}$$

The LHS of equation (29) must be strictly positive (for a nontrivial solution) hence we must have $b_\infty \neq b_{-\infty}$. From which it follows that we cannot have pulse waves and only front waves can exist for $\mu > 1$ when $\phi = 1$.

For $\mu > 1$, we can express equation (28) in the standard Fisher–Kolmogorov form [2,15] by writing

$$b = \left(\frac{\mu - 1}{\mu}\right)\overline{b}, \quad \overline{y} = (\mu - 1)^{1/2} y, \quad \nu = (\mu - 1)^{1/2}\overline{\nu}, \tag{30}$$

from which we obtain a minimum wave speed $\overline{\nu}_{\min} = 2$ and hence

$$\nu_{\min} = 2\sqrt{\mu - 1}. \tag{31}$$

This leads us to consider the wave speed for general values of the parameters.

4.2. Wave speed

Previous studies of travelling waves in quadratic autocatalytic systems, [5,6] for example, show that the propagation speed is determined from the behaviour of the solution at the front of the wave where $a \approx 1$, and b is small. The same considerations apply here. Linearizing equation (24) for b small leads to an equation for b which has solution of the form $\mathrm{e}^{-\lambda y}$, where

$$\lambda^2 - \nu\lambda + (\mu - \phi) = 0. \tag{32}$$

We require λ to be real (and positive); complex values for λ give rise to focal behaviour as $y \to \infty$, which, in turn, leads to ranges of y over which b would take negative values. Thus we must have

$$\nu \geqslant \nu_{\min} = 2\sqrt{\mu - \phi}. \tag{33}$$

Further, we can give an argument which follows very closely that given by Billingham and Needham [1] to show that the waves which will emerge as the long time solution to our initial-value problem will travel with the minimum speed, i.e., the propagation speed $c(t)$ of the waves formed from the initial-value problem (6)–(11) is such that $c(t) \to \nu_{\min}$ as $t \to \infty$. This will also be confirmed from the numerical integrations of the initial-value problem discussed below.

4.3. *Solution for ϕ large*

To obtain a solution to equations (23) and (24) valid for ϕ large, we first put $\mu = \mu_0\phi$, where μ_0 is O(1) as suggested by condition (22). We start by considering the region at the front of the wave, where we put $Y = \sqrt{\phi}\, y$, $V = \sqrt{\phi}\, \nu$ and leave a and b unscaled. Equations (23) and (24) become

$$\frac{\mathrm{d}^2 a}{\mathrm{d}Y^2} + V\frac{\mathrm{d}a}{\mathrm{d}Y} + \frac{1}{\phi}(1-a) - \mu_0 ab = 0, \tag{34}$$

$$\frac{\mathrm{d}^2 b}{\mathrm{d}Y^2} + V\frac{\mathrm{d}b}{\mathrm{d}Y} + \mu_0 ab - b = 0. \tag{35}$$

Equations (34) and (35) suggest looking for a solution by expanding

$$a = a_0 + \phi^{-1}a_1 + \phi^{-2}a_2 + \cdots, \tag{36a}$$

$$b = b_0 + \phi^{-1}b_1 + \phi^{-2}b_2 + \cdots, \tag{36b}$$

$$V = V_0 + \phi^{-1}V_1 + \phi^{-2}V_2 + \cdots. \tag{36c}$$

The leading order problem is

$$a_0'' + V_0 a_0' - \mu_0 a_0 b_0 = 0, \tag{37}$$

$$b_0'' + V_0 b_0' + \mu_0 a_0 b_0 - b_0 = 0 \tag{38}$$

with

$$a_0 \to 1, \quad b_0 \to 0 \quad \text{as } Y \to \infty$$

(where primes denote differentiation with respect to Y).

Now with $V_0 = \overline{V}_0\sqrt{\mu_0}$, $\overline{Y} = Y\sqrt{\mu_0}$, equations (37) and (38) become

$$a_0'' + \overline{V}_0 a_0' - a_0 b_0 = 0, \tag{39}$$

$$b_0'' + \overline{V}_0 b_0' + a_0 b_0 - \frac{b_0}{\mu_0} = 0. \tag{40}$$

This system is discussed in detail in [6], where it is shown that these equations have a solution only if $\mu_0 > 1$ and have

$$b_0 \to 0, \quad a_0 \to a_s(\mu_0) \quad \text{as } Y \to -\infty,$$

where $\mu_0 a_s < 1$, i.e., $a_s < 1$, and with a_s being determined numerically from the solution of equations (39) and (40).

We now consider the problem at O(ϕ^{-1}), namely,

$$a_1'' + V_0 a_1' + V_1 a_0' - \mu_0(a_0 b_1 + a_1 b_0) + 1 - a_0 = 0, \tag{41}$$

$$b_1'' + V_0 b_1' + V_1 b_0' + \mu_0(a_0 b_1 + a_1 b_0) - b_1 = 0 \tag{42}$$

with

$$a_1 \to 0, \quad b_1 \to 0 \quad \text{as } Y \to \infty.$$

The solution to this linear problem is not important for our discussion, only the behaviour as $Y \to -\infty$ is required. We find that

$$a_1 \approx -\frac{(1-a_s)}{V_0} Y + \cdots, \quad b_1 \to 0 \quad \text{as } Y \to -\infty. \tag{43}$$

A consideration of the problem at O(ϕ^{-2}) shows that

$$a_2 \approx -\frac{(1-a_s)}{2V_0^2} Y^2 - V_1 \frac{(1-a_s)}{V_0^2} Y + \cdots, \quad b_2 \to 0 \quad \text{as } Y \to -\infty. \tag{44}$$

Hence we have

$$b \to 0,$$
$$a \approx a_s - \frac{(1-a_s)}{V_0} Y\phi^{-1} - \frac{(1-a_s)}{2V_0^2} Y^2 \phi^{-2} - V_1 \frac{(1-a_s)}{V_0^2} Y\phi^{-2} + \cdots. \tag{45}$$

Expression (45) shows that expansion (36) becomes non-uniform when Y is O(ϕ). This leads us to consider a further region at the rear of the wave in which $b \equiv 0$, a is O(1) and where we put $\zeta = y/\sqrt{\phi}$. This results in the equation

$$\frac{1}{\phi} \frac{\mathrm{d}^2 a}{\mathrm{d}\zeta^2} + V \frac{\mathrm{d}a}{\mathrm{d}\zeta} + 1 - a = 0.$$

A solution in inverse powers of ϕ is suggested. The leading order term $a_0(\zeta)$ is given by

$$a_0(\zeta) = 1 - (1 - a_s)\mathrm{e}^{\zeta/V_0}$$

on matching with (45), from which it follows that

$$a_0 \to 1 \quad \text{as } \zeta \to -\infty. \tag{46}$$

The result in (46) leads us to the conclusion that, for ϕ large, we should expect to see pulse waves. However, an examination of the kinetics of the system shows that this stationary state is unstable. Therefore, we expect that, after a large initial perturbation generated by the passage of the wave, the concentrations of A and B will slowly approach the stable stationary state (15), over a region where diffusive effects will generally be negligible.

A consideration of equations (12) and (13) for ϕ large suggests that, when (15) has a focal character, this approach will have a two-time behaviour. There will be relatively narrow regions where the concentration of A changes rapidly and that of B goes through a non-trivial excursion, and much wider regions where the concentration of A increases slowly with that of B remaining small and close to its stationary state value, which, in this context, is of O(ϕ^{-1}). To illustrate this response we plot, in figure 3a, the trajectories in the (a, b) phase plane, for a solution for ϕ large (here $\mu = 1000,\ \phi = 800$) starting close $(a, b) = (1, 0)$. The corresponding time responses for a and b are shown in figures 3b and 3c. Finally, we note that the analysis developed above for ϕ large holds for μ_0 large, reducing to the standard Fisher–Kolmogorov problem ([1,2], for example) as $\mu_0 \to \infty$. Consequently, no further asymptotic scalings for μ are required and the discussion of this case is complete. We are now in a position to consider the numerical solutions to the full initial-value problem.

5. Numerical solutions

The numerical solution scheme used to solve the IVP represented by equations (6)–(11) is based on the Crank–Nicolson method, and used the Newton–Raphson method to solve the systems of non-linear finite-difference equations that arise at each time step. Choleski decomposition was used to invert the matrices. This solution scheme incorporates a time-step check to maintain accuracy and is described fully in [5]. It has been used successfully on a series of similar initial value problems, for example, in [6–9].

The computations were performed over a domain large enough to allow permanent form travelling waves to be generated. At both ends of the domain zero-flux boundary conditions were applied. For the initial perturbation we took $g(x) = 1$ for $0 \leqslant x < 1$, with a value of $b_0 = 0.5$. Typically we used 2000 points in the space variable and a step size $\Delta x = 0.1$. Numerical solutions were obtained for a range of values of μ and ϕ and the integrations were performed until a wave of permanent form had evolved. This was monitored by calculating the wave speed and the computations were continued until this was seen to be approaching a constant value.

Initially, calculations were performed with $\mu < \phi$ and in all cases tried no waves were seen to form, as expected. Here the concentration of B quickly became zero and that of A then returned to unity slowly through diffusive effects. We next performed numerical integrations with $\mu > \phi$. Here a travelling wave of permanent form was seen to evolve in all cases. The asymptotic (large time) value of the speed of these waves closely correlated (to within our numerical accuracy) with $\nu_{\min}$ as given by (33).

For relatively small values of μ and ϕ, (figure 4, for $\mu = 1$ and $\phi = 0.2$, 0.5, 0.8) the wave profiles remain monotone throughout and have the standard front wave appearance seen in many autocatalytic systems.

As μ is increased, (figure 5, $\mu = 10$, $\phi = 2$, 5, 8) the wave profiles are no longer monotone, now there is an increase in b and a decrease in a before the stable stationary state (15) is attained at the rear of the wave. This trend becomes more pronounced as

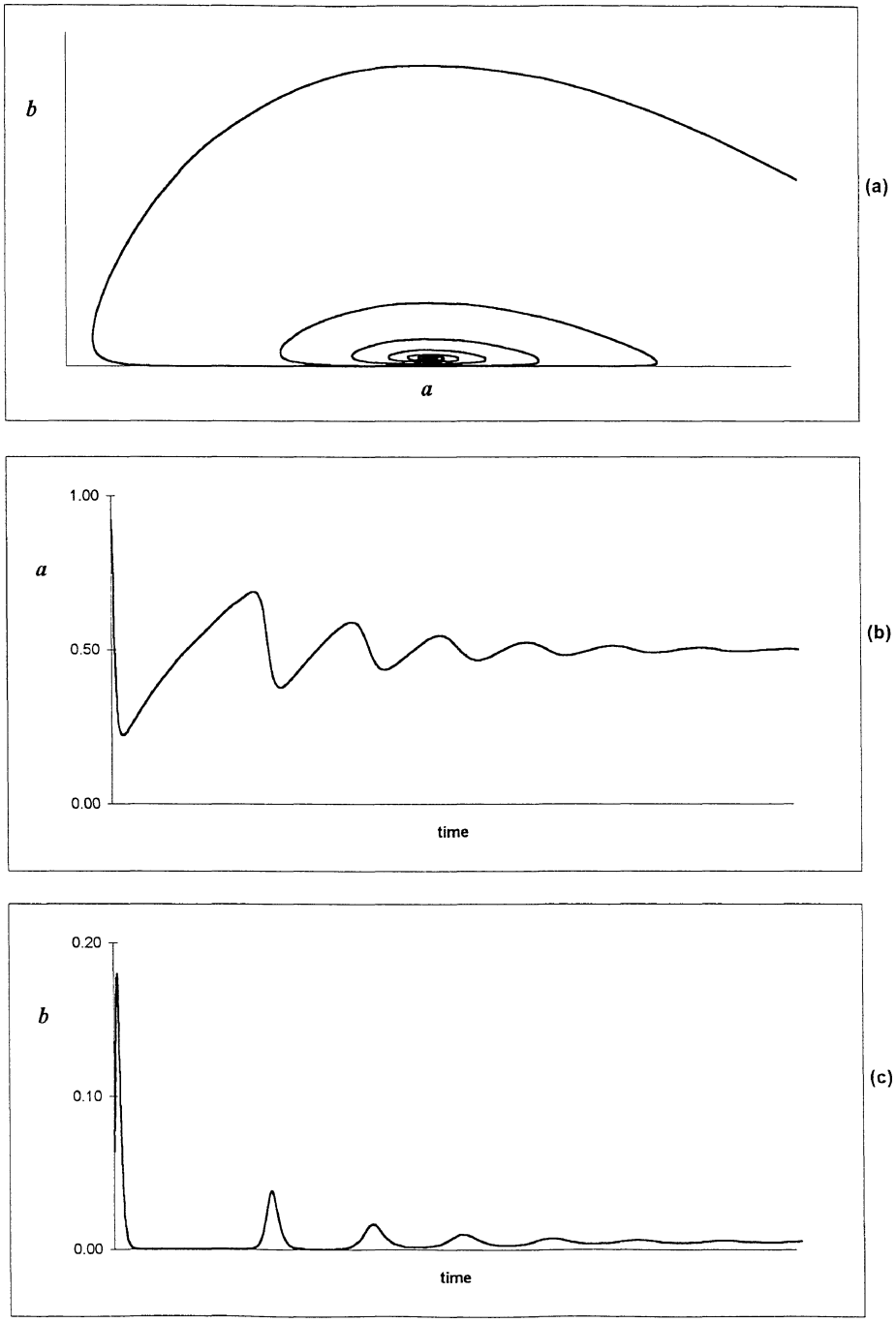

Figure 3. Solution of the kinetic equations (12) and (13) for $\mu = 1000$ and $\phi = 800$, starting close to the unstable stationary state $(a, b) = (1, 0)$: (a) phase plane, (b) time response for a, (c) time response for b.

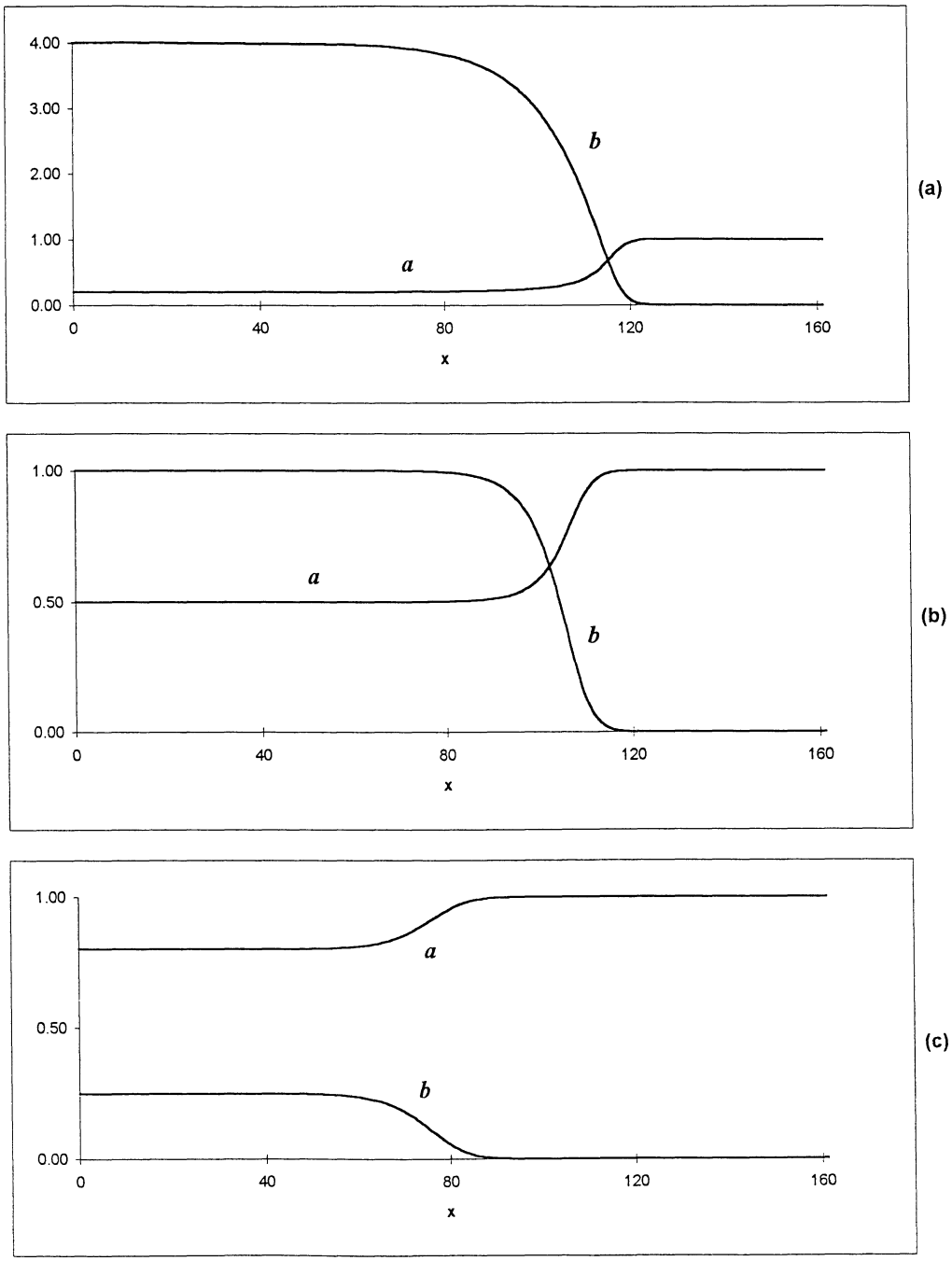

Figure 4. Wave profiles obtained from numerical integration of the full IVP, for $\mu = 1.0$ and (a) $\phi = 0.2$, (b) $\phi = 0.5$, (c) $\phi = 0.8$.

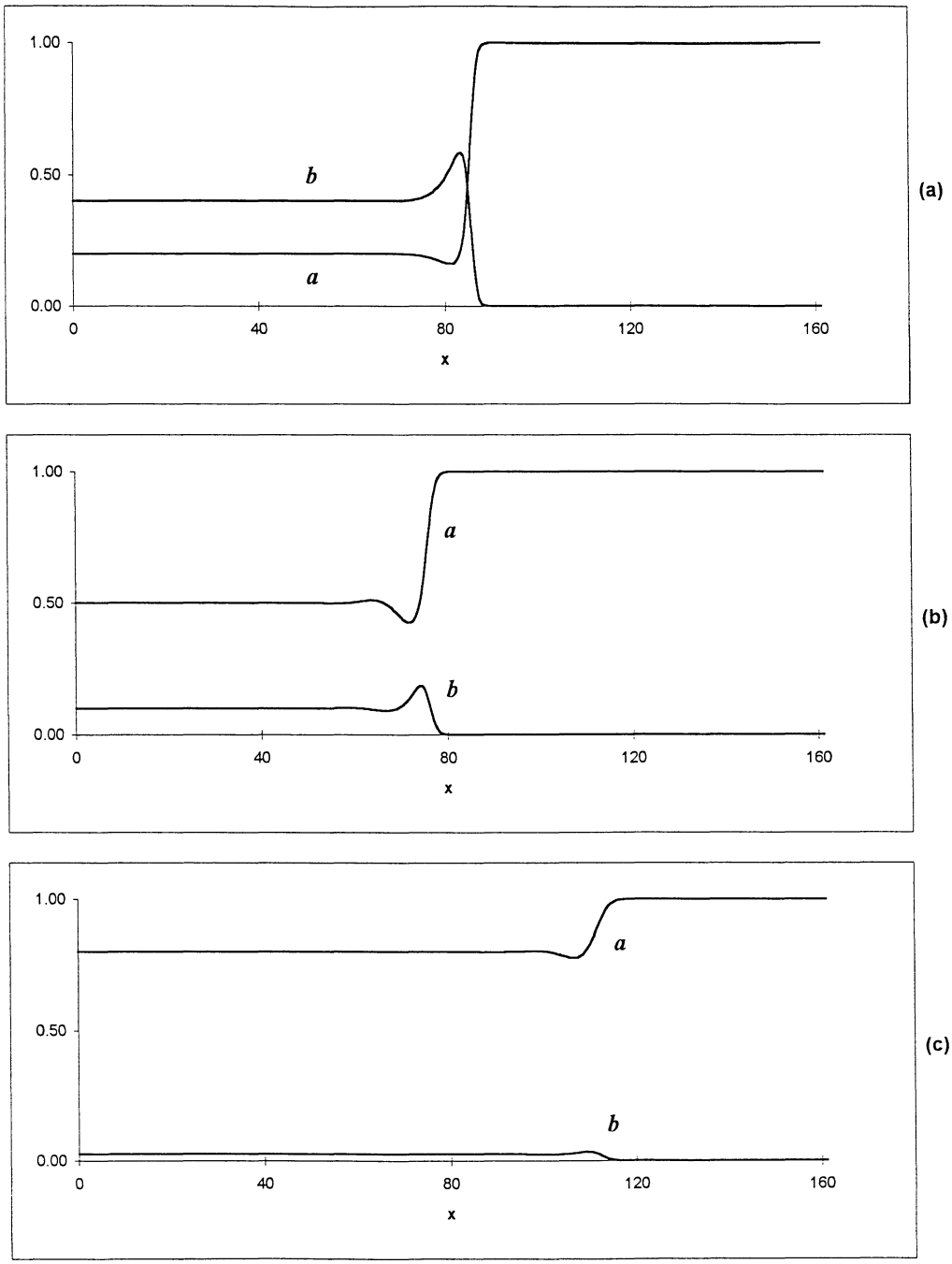

Figure 5. Wave profiles obtained from numerical integration of the full IVP, for $\mu = 10$ and (a) $\phi = 2$, (b) $\phi = 5$, (c) $\phi = 8$.

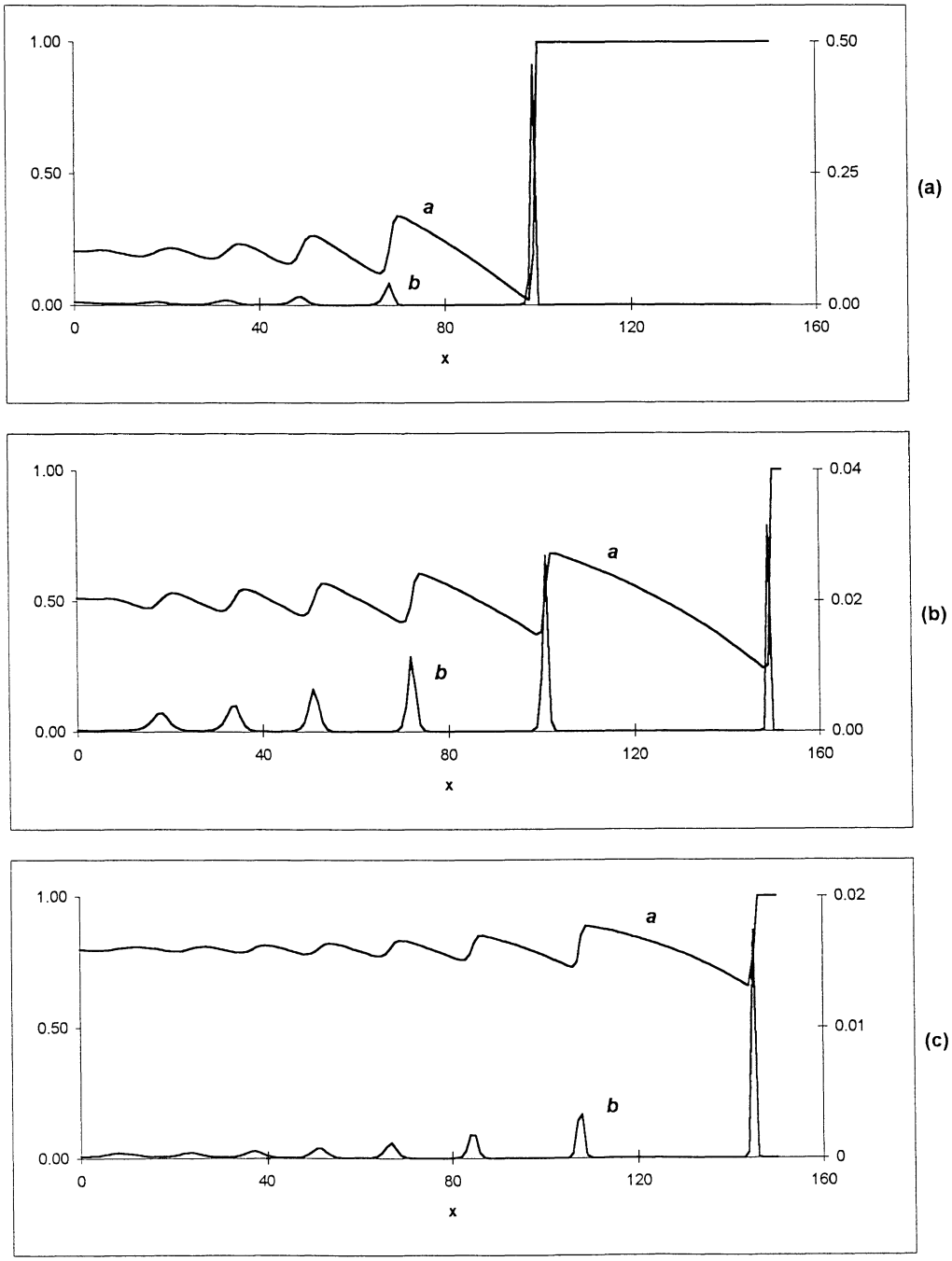

Figure 6. Wave profiles obtained from numerical integration of the full IVP, for $\mu = 1000$ and (a) $\phi = 200$, (b) $\phi = 500$, (c) $\phi = 800$.

μ is increased, and by $\mu = 1000$ (figure 6) a long lived transient behaviour is seen at the rear of the wave. This follows closely the behaviour seen in the solution of the kinetic equations (12, 13) for μ and ϕ large. Note that for $\phi = 500$ and more so for $\phi = 800$, there are very small responses in b (note the different scales for the plots of a and b in figure 6) and that these small responses produce very much larger variations in the concentration of A after the passage of the initial wave front.

6. Conclusions

We have considered an open isothermal reaction–diffusion system with quadratic autocatalytic kinetics. The permanent form travelling waves generated in the system by some local input of autocatalyst have been examined. From examination of the kinetics we found that stationary state (14) is a stable node for $\mu < \phi$ and unstable otherwise. The stationary state (15) was found to be stable and attractive for $\mu > \phi$ and unstable otherwise.

From examination of a priori bounds for the full initial value problem we established that a necessary condition for travelling waves to exist is that $\mu \geqslant \phi$.

Analysis of the permanent form travelling wave equations showed that, under the necessary condition, travelling waves with monotone profile are generated for solutions with $\phi = 1$. Solutions for larger values of μ and ϕ, however, can exhibit an oscillatory approach to the stationary state, ultimately controlled by the kinetics of the system. The nature of these oscillations has been shown to be a succession of rapid reactions, followed by gradual recovery of the concentration a until the next reaction is triggered. The concentration b exhibits short-lived but significant increases, corresponding to the local minima in concentration a. We believe that this transient 'pseudo' pulse wave behaviour in B and the ramp-like oscillatory approach to the stationary state of A, is the only complex behaviour which can be found in the quadratic autocatalysis system we have studied under the condition of equality of diffusivities.

References

[1] J. Billingham and D.J. Needham, The development of travelling waves in quadratic and cubic autocatalysis with unequal diffusion rates. III. Large time development in quadratic autocatalysis, Quart. Appl. Math. L (1992) 343–372.

[2] N.F. Britton, *Reaction–Diffusion Equations and Their Applications to Biology* (Academic Press, 1986).

[3] W.B. Jones and J.J. O'Brien, Pseudo-spectral methods and linear instabilities in reaction–diffusion fronts, Chaos 6 (1996) 219–228.

[4] K.J. Lee, W.D. McCormick, J.E. Pearson and H.L. Swinney, Experimental observations of self-replicating spots in a reaction–diffusion system, Nature 369 (1994) 215–218.

[5] J.H. Merkin and D.J. Needham, Propagating reaction–diffusion waves in a simple isothermal autocatalytic chemical system, J. Engineering Math. 23 (1989) 343–356.

[6] J.H. Merkin and D.J. Needham, The development of travelling waves in a simple isothermal chemical system. I. Quadratic autocatalysis with linear decay, Proc. R. Soc. Lond. A424 (1989) 187–209.

[7] J.H. Merkin, D.J. Needham and S.K. Scott, Coupled reaction–diffusion waves in an isothermal autocatalytic chemical system, IMA J. Applied Math. 50 (1993) 43–76.
[8] J.H. Merkin, V. Petrov, S.K. Scott and K. Showalter, Wave-induced chemical chaos, Phys. Rev. Letters 76 (1996) 546–549.
[9] J.H. Merkin, V. Petrov, S.K. Scott and K. Showalter, Wave-induced chaos in a continuously fed unstirred reactor, J. Chem. Soc., Faraday Trans. 92(16) (1996) 2911–2918.
[10] J.H. Merkin and M.A. Sadiq, The propagation of travelling waves in an open cubic autocatalytic chemical system, IMA J. Applied Math. 57 (1996) 273–309.
[11] J.E. Pearson, Complex patterns in a simple system, Science 261 (1993) 189–192.
[12] V. Petrov, S.K. Scott and K. Showalter, Excitability, wave reflection and wave splitting in a cubic autocatalysis reaction–diffusion system, Phil. Trans. R. Soc. Lond. A347 (1994) 631–642.
[13] K.E. Rasmussen, W. Mazin, E. Mosekilde, G. Dewel and P. Borekmans, Wave-splitting in the bistable Gray–Scott Model, Int. J. Bifurcation and Chaos 6 (1996) 1077–1092.
[14] W.N. Reynolds, J.E. Pearson and S. Ponce-Dewson, Dynamics of self-replicating patterns in reaction–diffusion systems, Phys. Rev. Letters 72 (1994) 2797–2800.
[15] A. Saul and K. Showalter, *Oscillations and Travelling Waves in Chemical Systems*, eds. R.J. Field and M. Burger (Wiley, New York, 1985) chapter 11.
[16] J. Smoller, *Shock Waves and Reaction–Diffusion Equations* (Springer, 1983).